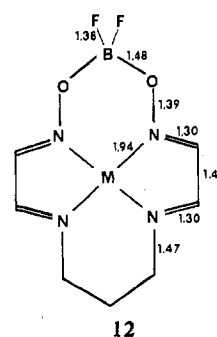


the oxidation state of the metal, its coordination number, the nature of the macrocyclic ligand, and indeed the finer details of its geometry. In molecular orbital terms the reasons for such behavior lie first with the presence of low-lying (usually π -type) orbitals in the macrocycles and second with relatively deep-lying metal d orbitals at this end of the periodic table. (For gallium, two elements further along in the periodic table, we seldom consider the 3d orbitals when looking at its chemistry: they are usually considered to be buried in the core.) It is interesting to speculate that this internal electron-transfer process, which may be tailored by adjustment of the variables, we have just mentioned plays an important role in the molecular mechanism for electron transport in copper-containing proteins. Unfortunately at present there is no detailed description of the role of the copper site available to examine this idea further.

Acknowledgment. This work was initiated during conversations with R. R. Gagné, to whom we are grateful for access to unpublished data on these systems. We thank the Dreyfus Foundation for a Summer Fellowship (P.D.W.).

Appendix

Our calculations were carried out on molecule **12** with the dimensions given. It differs from the ligand used in the experimental work by replacement of some terminal alkyl groups by H atoms. The parameters of the extended Hückel calculations¹⁷ are given in Table III. The calculations are of course rather crude ones, and the position of the $x^2 - y^2$ orbital will



be sensitive to the actual choice of exponents and coefficients as in any calculation. Use of an arbitrary single- ζ radial 3d function gave an orbital description qualitatively similar to that described in the paper. The $x^2 - y^2$ orbital dropped in energy as the (single) exponent increased in these calculations. The Richardson et al. double- ζ functions,¹⁸ with which we obtained the results described, needed to be employed to distinguish quantitatively, for example, between isoelectronic Ni^I and Cu^{II}. Values of the metal 4s and 4p orbital exponents and s, p, and d VSIP's are those used by Hoffmann and Mehrotra.⁹ Bond lengths for the other molecules studied were similar to those of **12**. In the carbonyl adducts M-CO = 1.78 Å and C-O = 1.12 Å.

Registry No. LBF₂, 74219-94-6; Cu, 7440-50-8; Ni, 7440-02-0.

(17) R. Hoffmann, *J. Chem. Phys.*, **39**, 1397 (1963).

(18) J. W. Richardson, W. C. Nieuwpoort, R. R. Powell, and W. E. Edgell, *J. Chem. Phys.*, **36**, 1057 (1962).

Contribution from the Department of Chemistry,
Purdue University, West Lafayette, Indiana 47907

Stability and Kinetics of a Macrocyclic Tetrapeptide Complex, Tetradeprotonated (*cyclo*-(β -Alanyl-glycyl- β -alanyl-glycyl))cuprate(II)

JAMES S. RYBKA and DALE W. MARGERUM*

Received January 3, 1980

The 14-membered macrocyclic ligand *cyclo*-(β -alanyl-glycyl- β -alanyl-glycyl) (C) reacts with copper(II) and releases four protons in base to form Cu(H₄C)²⁻. The ESR spectrum at room temperature shows a finely resolved nitrogen fine structure and is consistent with a structure having four deprotonated peptide nitrogens in a planar arrangement about copper(II). A stability constant of log *K = -25.1 (for the reaction Cu²⁺ + C \rightleftharpoons Cu(H₄C)²⁻ + 4H⁺) is determined by competition with triethylenetetramine (trien). The rate of reaction of Cu(H₄C)²⁻ with trien is many orders of magnitude slower than that of other copper(II)-peptide complexes. The kinetics of the trien reaction corresponds to a reaction sequence in which protonation by solvent, coordination by trien, and a second protonation by solvent are required to displace the macrocyclic ligand. The acid-dissociation rates are also relatively slow. The rate-determining step is proton transfer to a peptide nitrogen with a rate constant of 6.2 \times 10⁵ M⁻¹ s⁻¹ for H₃O⁺ and 4.6 \times 10³ M⁻¹ s⁻¹ for CH₃COOH. Above pH 5 a higher order hydrogen ion dependence is observed.

Introduction

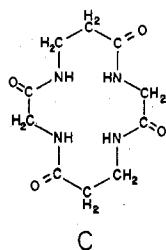
Oligopeptides react with copper(II) ion to form complexes in which the peptide nitrogen atoms deprotonate and coordinate to the metal. Potentiometric,¹⁻³ spectrophotometric,³ and crystallographic⁴ methods have been used to establish the

structure and thermodynamic stabilities of these complexes. The kinetics and mechanisms have been studied for many copper-peptide reactions.⁵⁻¹¹

(1) Manyak, A. R.; Murphy, C. B.; Martell, A. E. *Arch. Biochem. Biophys.* **1955**, *59*, 373-382.
 (2) Dobbie, H.; Kermack, W. O. *J. Biochem. (Tokyo)* **1955**, *59*, 257-264.
 (3) Kim, M. K.; Martell, A. E. *J. Am. Chem. Soc.* **1966**, *88*, 914-918.
 (4) Freeman, H. C. In "The Biochemistry of Copper"; Peisach, J., Aisen, P., Blumberg, W. E., Eds.; Academic Press: New York, 1966.

(5) Margerum, D. W.; Dukes, G. R. In "Metals Ions in Biological Systems"; Sigel, H., Ed.; Marcel Dekker: New York, 1974; Vol. 1, Chapter 5, pp 157-212.
 (6) Margerum, D. W.; Wong, L. F.; Bossu, F. P.; Chellappa, K. L.; Czarnecki, J. J.; Kirksey, S. T., Jr.; Neubecker, T. A. *Adv. Chem. Ser.* **1977**, No. 162, 281-303.
 (7) Bannister, C. B.; Margerum, D. W.; Raycheba, J. M. T.; Wong, L. F. *Symp. Faraday Soc.* **1975**, *10*, 78-88.
 (8) Pagenkopf, G. K.; Margerum, D. W. *J. Am. Chem. Soc.* **1968**, *90*, 501.

This work introduces a novel copper-peptide complex in which the ligand is a cyclic tetrapeptide, *cyclo*-(β -alanyl-glycyl- β -alanyl-glycyl) (C). Cyclic tetra- and hexapeptides



have been studied by circular dichroism and nuclear magnetic resonance in order to determine the conformations of larger naturally occurring cyclic peptides.¹² The macrocyclic peptide ligands are known to coordinate via peptide oxygens to group 1 and 2 metals,^{13,14} but this is the first report of coordination to a transition metal via peptide nitrogens.

In contrast to other copper(II)-peptide complexes, the macrocyclic ligand lacks both the amine and carboxylate terminals. As a consequence relatively high pH (>13) is needed to form the complex, yet once formed the copper complex is stable down to pH 8. Unlike the group 1 and 2 metals, copper(II) goes to the center of the macrocycle. The stoichiometry shows that four protons are released in forming the complex. The visible and ESR spectra indicate that copper(II) is coordinated to four deprotonated peptide nitrogens consistent with a $\text{Cu}(\text{H}_4\text{C})^{2-}$ species. The formation constant of this complex was determined by competition with triethylenetetramine. The kinetics of the trien and acid reactions of $\text{Cu}(\text{H}_4\text{C})^{2-}$ show that steric considerations of the macrocycle impart a kinetic stability, making ligand displacement much slower than for open-chain peptides.

Experimental Section

Reagents. Copper(II) perchlorate was prepared by the reaction of copper(II) carbonate with perchloric acid. After recrystallization, a stock solution was prepared and standardized by EDTA titration with murexide indicator.

The ligand, *cyclo*-(β -alanyl-glycyl- β -alanyl-glycyl), was synthesized by Biosynthetika in Oberdorf, Switzerland, according to the method of Schwyzer¹⁵ as modified by Grathwohl.¹⁶ A ninhydrin test showed the sample to be free of linear peptide impurities. Anal. Calcd for $\text{C}_{10}\text{H}_{16}\text{N}_4\text{O}_4 \cdot 5/2\text{H}_2\text{O}$: C, 39.87; H, 6.98; N, 18.60. Found: C, 39.83; H, 6.98; N, 18.60. The solubility of the ligand in 0.1 M NaOH was determined to be 0.96 mg/mL (3.2×10^{-3} M), and hydrolysis after about 6 h in this media is negligible.

Proton magnetic resonance using a Perkin-Elmer R-32 spectrometer at room temperature confirmed the identity of the ligand. The spectrum of a 0.01 M ligand solution in trifluoroacetic acid consists of the following sets of peaks downfield of Me_4Si : a triplet at 7.75 ppm from the protons on the peptide nitrogens, a doublet at 4.10 ppm due to the protons on the glycyl residues, and a triplet and a hexet at 3.70 and 2.75 ppm, respectively, from the protons on the β -alanyl residues. The relative intensities of all these peaks are equal. Com-

parison with the proton NMR of *cyclo*-tetraglycyl supports this assignment.¹⁶

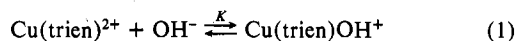
The copper(II)-macrocyclic tetrapeptide complex was formed in 10–15 min by adding freshly precipitated $\text{Cu}(\text{OH})_2$ to a slurry of the ligand in 0.1 M NaOH. Less time was needed to form the complex when higher concentrations of NaOH were used. Lyophilizing the solution to a minimal volume and storing in a vacuum desiccator for several days produced crystals. Decanting the mother liquor and washing with anhydrous ethanol resulted in a neutral powder. Anal. Calcd for $\text{Na}_2\text{Cu}(\text{C}_{10}\text{H}_{12}\text{N}_4\text{O}_4) \cdot 6\text{H}_2\text{O}$: C, 25.56; H, 5.16; N, 11.93. Found: C, 25.65; H, 5.17; N, 12.01.

The pH of the solutions was adjusted with NaOH or HClO_4 . The ionic strength was maintained at 1.0 M with NaClO_4 , which had been prepared by the neutralization of Na_2CO_3 with HClO_4 followed by boiling to remove CO_2 and stored under mildly acidic conditions.

Triethylenetetramine (trien) was obtained as the neat liquid by vacuum distillation. In some cases the trien-4HCl salt was recrystallized from hot water/methanol. Stock solutions were made freshly before each use.

Apparatus. Electron spin resonance (ESR) spectra were obtained by using a Varian E-109, X-band ESR system modulated at 100 kHz and equipped with a Varian variable-temperature controller. Aqueous samples were studied at room temperature in an E-238 multipurpose cavity using a thin quartz cell, S-813 supplied by Scanco, Solvang, CA. Solutions were freeze-quenched by trapping in hexane in a dry ice/acetone bath with use of an Update Model 705 syringe ram instrument. Coupling constants and g values were determined by comparison of the experimental spectrum to one generated on a computer.¹⁷ The magnetic field was calibrated with DPPH (1,1-diphenyl-2-picrylhydrazyl) in KCl embedded in paraffin. The visible spectrum was obtained with a Cary 14 spectrophotometer. The solution pH was determined by using the Instrumentation Laboratory Model 245 pH meter with a NaCl-saturated standard calomel reference electrode. This electrode system was calibrated for ionic strength correction by a pH titration of HClO_4 with standard NaOH; it was observed that $-\log [\text{H}^+] = \text{pH} + 0.29$ at $\mu = 1.0$ M (NaClO_4). All measurements were conducted at 25.0 °C and $\mu = 1.0$ M (NaClO_4) unless otherwise noted.

Equilibrium Measurements. The stability constant of the copper(II)-macrocyclic peptide complex was determined by competition with trien. Solutions of $\text{Cu}(\text{H}_4\text{C})^{2-}$ were mixed with excess trien, adjusted in pH, and allowed to equilibrate for several days before the spectra were recorded. The two complexes have different spectral properties, and so their equilibrium concentrations can be assayed at two wavelengths on opposite sides of the isosbestic at 490 nm. The spectral properties of $\text{Cu}(\text{trien})^{2+}$ are pH dependent and must be corrected for the equilibrium of eq 1, for which $\log K = 1.2$.¹⁸



Kinetic Measurements. The kinetics of the trien reactions were followed by using a Cary 16 spectrophotometer interfaced to an Intel 8008 microprocessor through an Analog Devices analog to digital converter. Data reduction was done off-line by using a linear and nonlinear regression analysis on a Hewlett-Packard 2115A (8K, 16 bit) general-purpose computer. The absorbance change due to the formation of $\text{Cu}(\text{trien})^{2+}$ was monitored at 580 nm. trien and standard NaOH were in excess over the complex. Excellent pseudo-first-order kinetics were obtained under these conditions with the observed rate constant, k_{obsd} , defined as in eq 2.

$$d[\text{Cu}(\text{trien})^{2+}]/dt = k_{\text{obsd}}[\text{Cu}(\text{H}_4\text{C})^{2-}] \quad (2)$$

The acid-dissociation reactions of $\text{Cu}(\text{H}_4\text{C})^{2-}$ were studied on a Durrum stopped-flow spectrophotometer interfaced to the HP2115A computer.¹⁹ Acetate and PIPES (piperazine- N,N' -bis(2-ethanesulfonic acid)) buffers were used to control the pH. The absorbance change at 250 nm due to the loss of $\text{Cu}(\text{H}_4\text{C})^{2-}$ was first order with an observed rate constant defined by eq 3.

$$-d[\text{Cu}(\text{H}_4\text{C})^{2-}]/dt = k_{\text{obsd}}[\text{Cu}(\text{H}_4\text{C})^{2-}] \quad (3)$$

- (9) Pagenkopf, G. K.; Margerum, D. W. *J. Am. Chem. Soc.* **1968**, *90*, 6963–6967.
 (10) Pagenkopf, G. K.; Margerum, D. W. *J. Am. Chem. Soc.* **1970**, *92*, 2683–2686.
 (11) Hauer, H.; Dukes, G. R.; Margerum, D. W. *J. Am. Chem. Soc.* **1973**, *95*, 3515–3522.
 (12) Deber, C. M.; Madison, V.; Blout, E. R. *Acc. Chem. Res.* **1976**, *9*, 106–113.
 (13) Madison, V.; Atreyi, M.; Deber, C. M.; Blout, E. R. *J. Am. Chem. Soc.* **1974**, *96*, 6725–6734.
 (14) Baron, D.; Pease, L. G.; Blout, E. R. *J. Am. Chem. Soc.* **1977**, *99*, 8299–8306.
 (15) Schwyzer, R.; Iselin, B.; Rittel, W.; Sieber, P. *Helv. Chim. Acta* **1956**, *39*, 872–883.
 (16) Grathwohl, C.; Tun-Kyi, A.; Bundi, A.; Schwyzer, R.; Wüthrich, K. *Helv. Chim. Acta* **1975**, *58*, 415–423.

- (17) Toy, A. D.; Chaston, S. H. H.; Pilbrow, J. R.; Smith, T. D. *Inorg. Chem.* **1971**, *10*, 2219–2226.
 (18) Carr, J. D.; Olsen, V. K. *Inorg. Chem.* **1975**, *14*, 2168–2174.
 (19) Willis, B.; Bittikofer, J. A.; Pardue, H. L.; Margerum, D. W. *Anal. Chem.* **1970**, *42*, 1340–1349.

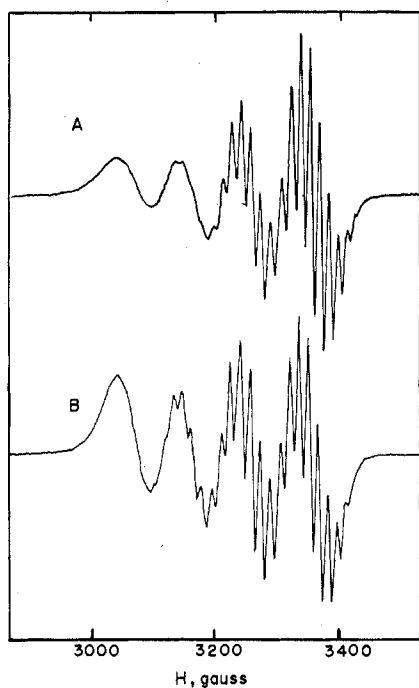


Figure 1. ESR spectrum of $\text{Cu}(\text{H}_4\text{C})^{2-}$ (the magnetic field was modulated at 100 kHz, $g_0 = 2.092$, $A(\text{Cu}) = 87.5 \text{ G}$ ($85.4 \times 10^{-4} \text{ cm}^{-1}$), and $A(\text{N}) = 14.0 \text{ G}$ ($13.7 \times 10^{-4} \text{ cm}^{-1}$)): (A) $[\text{Cu}(\text{H}_4\text{C})^{2-}] = 1.5 \times 10^{-3} \text{ M}$ in 0.024 M NaOH ($\mu = 1.0 \text{ M}$ (NaClO_4)) at 25 °C, $\nu = 9.392 \text{ GHz}$; (B) $[\text{Cu}(\text{H}_4\text{C})^{2-}] = 3.2 \times 10^{-3} \text{ M}$ in 0.10 M NaOH ($\mu = 1.0 \text{ M}$ (NaClO_4)) at 60 °C, $\nu = 9.288 \text{ GHz}$.

Results

The visible spectrum of $\text{Cu}(\text{H}_4\text{C})^{2-}$ is characterized by one peak with an absorbance maximum at 488 nm ($\epsilon 54 \text{ M}^{-1} \text{ cm}^{-1}$). The wavelength of the maximum is independent of $[\text{OH}^-]$ from pH 8.2 to pH 14.0.

The unpaired electron in the copper(II) complex with square-planar (or tetragonally elongated octahedral) geometry is in the $d_{x^2-y^2}$ orbital. The spin of the copper nucleus is $I = 3/2$, and that of nitrogen is $I = 1$. Four lines are observed in the room-temperature ESR for $\text{Cu}(\text{H}_4\text{C})^{2-}$ due to the copper coupling, and each of these should be split into nine due to the hyperfine coupling of the four nitrogens. Figure 1A presents the experimental ESR spectrum in 0.024 M NaOH at 25 °C; identical spectra are obtained in 1.0 M NaOH and at pH 8.15. The spectrum is characterized by $g_0 = 2.092$, $A_0(\text{Cu}) = 87.5 \text{ G}$ ($85.4 \times 10^{-4} \text{ cm}^{-1}$), and $A_0(\text{N}) = 14.0 \text{ G}$ ($13.7 \times 10^{-4} \text{ cm}^{-1}$). The line width for a paramagnetic ion in solution varies with field strength;²⁰ for this reason the nitrogen hyperfine lines are more clearly resolved on the high-field side of the spectrum. Other copper(II)-peptide complexes do not show this high degree of resolution. At 60 °C this resolution (Figure 1B) has been improved, suggesting that spin-tumbling effects are determining the line broadening.

The anisotropic ESR spectrum of $\text{Cu}(\text{H}_4\text{C})^{2-}$ was obtained at -150 °C with $[\text{Cu}(\text{H}_4\text{C})] = 2 \times 10^{-4} \text{ M}$ in 1.0 M NaClO_4 . At higher concentrations of complex and lower ionic strength, only one broad resonance is observed due to the Cu(II)-Cu(II) interactions which occur when regions of high Cu(II)-complex concentration separate out upon freezing.²¹ The following parameters characterize the spectrum: $g_{\perp} = 2.065$, $g_{\parallel} = 2.145$, $A_{\parallel}(\text{Cu}) = 230 \text{ G}$ ($230 \times 10^{-4} \text{ cm}^{-1}$), and $A_{\parallel}(\text{N}) = 14.5 \text{ G}$ ($14.0 \times 10^{-4} \text{ cm}^{-1}$). The calculated $\langle g \rangle = \frac{1}{3}g_{\parallel} + \frac{2}{3}g_{\perp} = 2.092$ in excellent agreement with the isotropic value. The nitrogen

Table I. Hydroxide Dependence of the Equilibrium Concentrations of $\text{Cu}(\text{H}_4\text{C})^{2-}$ and $\text{Cu}(\text{trien})^{2+}$ ^a

$-\log [\text{OH}^-]$	$10^3 [\text{Cu}(\text{H}_4\text{C})^{2-}]$, M	$10^3 [\text{Cu}(\text{trien})^{2+}]$, M	$\log ([\text{Cu}(\text{trien})^{2+}][\text{C}]/[\text{Cu}(\text{H}_4\text{C})^{2-}][\text{trien}])$
1.69	0.258	0.099	-2.368
1.78	0.211	0.150	-1.912
1.97	0.117	0.273	-1.132
2.06	0.082	0.317	-0.845

^a The solutions were buffered with trien; $[\text{trien}]_0 = 8.9 \times 10^{-3} \text{ M}$. $[\text{Cu}(\text{H}_4\text{C})]_0 = 3.8 \times 10^{-4} \text{ M}$, $\mu = 0.2 \text{ M}$ (NaClO_4), 25.0 °C.

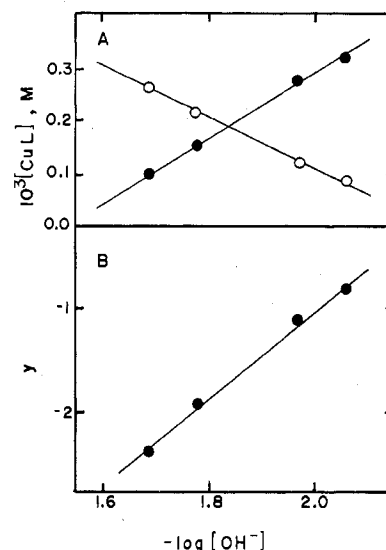
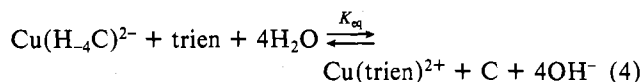


Figure 2. (A) Equilibrium concentrations of $\text{Cu}(\text{H}_4\text{C})^{2-}$ (O) and $\text{Cu}(\text{trien})^{2+}$ (●) as a function of $[\text{OH}^-]$ at $\mu = 0.2 \text{ M}$ (NaClO_4) and 25.0 °C with $[\text{trien}]_0 = 8.9 \times 10^{-3} \text{ M}$. (B) Dependence of the equilibrium of $\text{Cu}(\text{H}_4\text{C})^{2-}/\text{Cu}(\text{trien})^{2+}$ as a function of $[\text{OH}^-]$. The ordinate, y , is defined by eq 6; slope = 4; intercept = $\log K_{\text{eq}} = -9.3$.

hyperfine coupling constants for both temperatures agree within experimental error.

Stability Constant of $\text{Cu}(\text{H}_4\text{C})^{2-}$. The stability constant of the copper(II)-macrocylic peptide complex was determined by competition with trien:



The equilibrium concentrations of $\text{Cu}(\text{H}_4\text{C})^{2-}$ and $\text{Cu}(\text{trien})^{2+}$ as a function of hydroxide ion concentration are presented in Table I and Figure 2A. The equilibrium constant defined in eq 5 can be written in terms of eq 6 which is plotted in

$$K_{\text{eq}} = \frac{[\text{Cu}(\text{trien})^{2+}][\text{C}][\text{OH}^-]^4}{[\text{Cu}(\text{H}_4\text{C})^{2-}][\text{trien}]} \quad (5)$$

$$y = \log \left(\frac{[\text{Cu}(\text{trien})^{2+}][\text{C}]}{[\text{Cu}(\text{H}_4\text{C})^{2-}][\text{trien}]} \right) = m(-\log [\text{OH}^-]) + \log K_{\text{eq}} \quad (6)$$

Figure 2B. The slope, $m = 4$, verifies the stoichiometry of the reaction. The intercept yields an estimate of $\log K_{\text{eq}} = -9.3$. A better value for $\log K_{\text{eq}}$ is found by using Figure 2A. At $-\log [\text{OH}^-] = 1.835$, $[\text{Cu}(\text{trien})^{2+}] = [\text{Cu}(\text{H}_4\text{C})^{2-}] = [\text{C}]$ and $[\text{trien}]$ can be calculated. Thus eq 5 can be evaluated directly, $\log K_{\text{eq}} = -9.0$, in agreement with the intercept of Figure 2B. This calculation was made on the assumption that mixed-ligand complexes are negligible. This assumption is supported by the kinetics of the ligand-exchange reaction. Mixed com-

(20) McConnell, H. M. *J. Chem. Phys.* **1956**, *25*, 709-711.

(21) Gould, D. C.; Mason, H. S. *Biochemistry* **1967**, *6*, 801-809.

Table II. Observed Rate Constants for the Reaction of $\text{Cu}(\text{H}_4\text{C})^{2-}$ with trien^a

$10^3 \times [\text{OH}^-], \text{M}$	$10^3 \times [\text{trien}], \text{M}$	$10^4 \times k_{\text{obsd}}, \text{s}^{-1}$	$10^3 \times [\text{OH}^-], \text{M}$	$10^3 \times [\text{trien}], \text{M}$	$10^4 \times k_{\text{obsd}}, \text{s}^{-1}$
1.8	2.92	2.60	8.0	52.3	4.11
1.8	15.1	5.38	8.0	90.2	5.09
1.8	33.3	6.81	12.0	9.6	0.58
1.8	57.2	8.48	12.0	26.3	1.54
1.8	99.0	8.93	12.0	51.0	2.80
8.0	6.6	0.69	12.0	92.8	3.86
8.0	27.2	2.81			

^a $[\text{Cu}(\text{H}_4\text{C})^{2-}] = 1.5 \times 10^{-4} \text{ M}$, $25.0 \pm 0.1 \text{ }^\circ\text{C}$, 1.0 M NaClO_4 .

plexes are present only as steady-state intermediate species and are not in appreciable concentration. In addition, we have observed that both the visible and ESR spectra of $\text{Cu}(\text{H}_4\text{C})^{2-}$ are unchanged in the presence of excess trien.

The formation constant for $\text{Cu}(\text{H}_4\text{C})^{2-}$, $K_{\text{Cu}(\text{H}_4\text{C})}$, is readily obtained by using eq 7, noting that $\log K_{\text{Cu}(\text{trien})} = 20.9$.²²

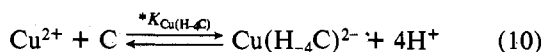
$$K_{\text{eq}} = \frac{K_{\text{Cu}(\text{trien})}}{K_{\text{Cu}(\text{H}_4\text{C})}} \quad (7)$$

$$K_{\text{Cu}(\text{H}_4\text{C})} = \frac{[\text{Cu}(\text{H}_4\text{C})^{2-}]}{[\text{Cu}^{2+}][\text{C}][\text{OH}^-]^4} = 10^{29.9} \quad (8)$$

Rearranging eq 8 in terms of $[\text{H}^+]$ and noting that $\log K_w = 13.76$ at 0.2 M NaClO_4 (determined by HClO_4 titration with NaOH), we obtained eq 9. The value of $*K_{\text{Cu}(\text{H}_4\text{C})}$ can be

$$*K_{\text{Cu}(\text{H}_4\text{C})} = K_{\text{Cu}(\text{H}_4\text{C})}K_w^4 = 10^{-25.1} \quad (9)$$

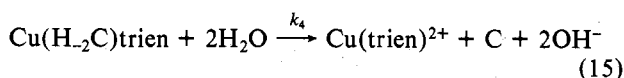
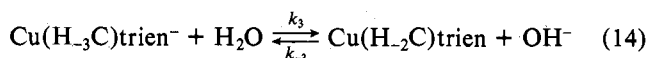
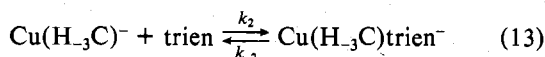
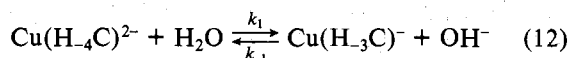
used to calculate the pH where dissociation of the complex becomes important. With the assumption of 10^{-3} M free ligand, the concentrations of Cu^{2+} and $\text{Cu}(\text{H}_4\text{C})^{2-}$ will be equal at pH 7. Direct measurement of the equilibrium in eq 10 is prevented by the hydrolysis and precipitation of copper.



Kinetics of the Reaction with trien. The kinetics of the reaction shown in eq 4 was studied as a function of trien and hydroxide ion concentrations. The rate of formation of $\text{Cu}(\text{trien})^{2+}$ at lower trien concentrations obeys the expression given in eq 11, where k has a complex hydroxide dependence.

$$\frac{d[\text{Cu}(\text{trien})^{2+}]}{dt} = k[\text{Cu}(\text{H}_4\text{C})^{2-}][\text{trien}] \quad (11)$$

At higher trien concentrations the rate becomes independent of trien. The observed first-order rate constants (eq 2) are summarized in Table II; Figure 3 shows the trien dependence at several hydroxide ion concentrations. The proposed mechanism for the reaction of $\text{Cu}(\text{H}_4\text{C})^{2-}$ with trien is described by eq 12–15. The series of equations (12)–(15)



represent the major pathway for the ligand exchange reaction.

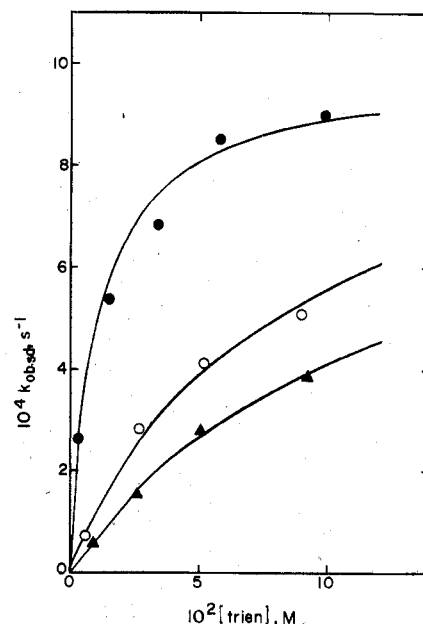


Figure 3. Dependence of k_{obsd} on trien concentration for the nucleophilic reactions of $\text{Cu}(\text{H}_4\text{C})^{2-}$. Solid lines were calculated from eq 16 with $k_1 = 9.9 \times 10^{-4} \text{ s}^{-1}$, $k_2/k_{-1} = 0.82$, $k_3/k_{-2} = 0.30$, and $k_4/k_{-3} = 7.8 \times 10^{-3} \text{ M}$. Conditions: $[\text{Cu}(\text{H}_4\text{C})^{2-}]_i = 1.5 \times 10^{-4} \text{ M}$, $\mu = 1.0 \text{ M}$ (NaClO_4), $25.0 \text{ }^\circ\text{C}$. $[\text{NaOH}]_i, \text{M}$: (●) 1.8×10^{-3} , (○) 8.0×10^{-3} , (▲) 12.0×10^{-3} .

Table III. Rate Constants for the Acid Dissociation of $\text{Cu}(\text{H}_4\text{C})^{2-}$ ^a

$-\log [\text{H}^+]$	$10^3 \times [\text{HB}]_T, \text{M}$	$k_{\text{obsd}}, \text{s}^{-1}$	$-\log [\text{H}^+]$	$10^3 \times [\text{HB}]_T, \text{M}$	$k_{\text{obsd}}, \text{s}^{-1}$
4.02	8.50	86.7	4.84	28.90	59.8
	17.00	120		42.50	87.2
	25.50	153		63.75	118.34
	42.50	220	5.25	25.50	17.43
	63.75	308		34.00	22.7
4.40	25.50	106		42.50	27.0
	34.00	131		63.75	39.7
	42.50	161	6.98	4.78 ^b	2.14×10^{-3}
	63.75	236		9.47 ^b	2.07×10^{-3}
4.84	8.50	24.0		21.80 ^b	7.32×10^{-3}
	19.25	42.1			

^a $\mu = 1.0 \text{ M}$ (NaClO_4), $T = 25.0 \text{ }^\circ\text{C}$, $[\text{Cu}(\text{H}_4\text{C})^{2-}]_0 = 3.0 \times 10^{-5} \text{ M}$, $\text{HB} = \text{acetic acid}$. ^b PIPES buffer.

Direct trien attack on $\text{Cu}(\text{H}_4\text{C})^{2-}$ is not observed. Instead this mechanism involves protonation of the complex by the solvent to form a $\text{Cu}(\text{H}_3\text{C})^-$ species, which is now able to react with trien. The resulting mixed complex reacts with solvent to become further protonated, $\text{Cu}(\text{H}_2\text{C})\text{trien}$. After the second protonation, trien is able to displace the cyclic peptide. The intermediates $\text{Cu}(\text{H}_3\text{C})^-$, $\text{Cu}(\text{H}_3\text{C})\text{trien}^-$, and $\text{Cu}(\text{H}_2\text{C})\text{trien}$ are all steady-state species. The observed first-order rate constant is described by eq 16, where $A = k_4/k_{-3}$, $B = k_3/k_{-2}$, and $C = k_2/k_{-1}$.

$$k_{\text{obsd}} = \frac{k_1 ABC [\text{trien}]}{[\text{OH}^-]^2 + A(1+B)[\text{OH}^-] + ABC [\text{trien}]} \quad (16)$$

The data in Table III were fit to eq 16 by using a nonlinear iterative procedure. The curves in Figure 3 were calculated by using the values $k_1 = 9.9 \times 10^{-4} \text{ s}^{-1}$, $k_2/k_{-1} = 0.82$, $k_3/k_{-2} = 0.30$, and $k_4/k_{-3} = 7.8 \times 10^{-3} \text{ M}$. The direct trien attack on $\text{Cu}(\text{H}_4\text{C})^{2-}$ is negligible (i.e., the rate constant for such a pathway is less than $10^{-5} \text{ M}^{-1} \text{ s}^{-1}$).

In fitting the kinetic data to a mechanism we were surprised to find that only a specific sequence of the type given in eq 12–15 was suitable. Several other simpler kinetic schemes were

(22) Martell, A. E.; Chaberek, S., Jr.; Westerback, S.; Hyytiainen, H. J. *Am. Chem. Soc.* 1957, 79, 3036–3041.

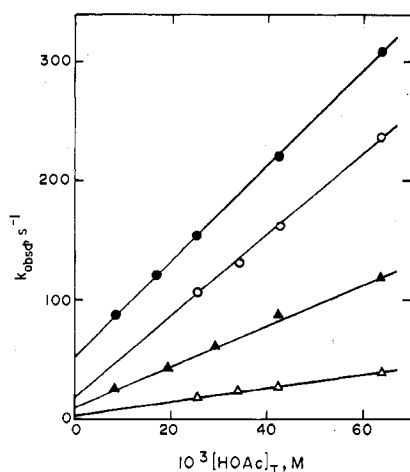


Figure 4. Dependence of k_{obsd} on $[\text{HOAc}]_{\text{T}}$ for the acid dissociation of $\text{Cu}(\text{H}_4\text{C})^{2-}$. Conditions: $[\text{Cu}(\text{H}_4\text{C})^{2-}]_i = 3.0 \times 10^{-5} \text{ M}$, $\mu = 1.0 \text{ M}$ (NaClO_4), $25.0 \text{ }^\circ\text{C}$; pH (●) 4.04, (○) 4.40, (▲) 4.80, (△) 5.26.

Table IV. Resolved Acid-Dissociation Rate Constants for $\text{Cu}(\text{H}_4\text{C})^{2-}$ ^a

$-\log [\text{H}^+]$	$10^{-3}k_{\text{HOAc}}$, $\text{M}^{-1} \text{s}^{-1}$	k'_{obsd} , s^{-1} ^b
4.08	5.1	52
4.40	5.5	17
4.84	4.7	10
5.25	3.1	2.7

^a $\mu = 1.0 \text{ M}$ (NaClO_4), $T = 25.0 \text{ }^\circ\text{C}$. ^b k'_{obsd} defined in eq 21.

attempted but would not fit the data. Any proposed scheme is subject to the following requirements. At high trien concentrations, k_{obsd} must become independent of trien, and the trien concentration at which this leveling off occurs must be a function of $[\text{OH}^-]$. At low trien concentrations, the trien dependence of k_{obsd} must show a mixed-order OH^- suppression. These constraints require that two of the proposed reactions must involve the release of OH^- and a third reaction must be one of the steady-state intermediates with trien.

A reasonable kinetic fit was obtained when the scheme included a preequilibrium to release OH^- , followed by the formation of a steady-state intermediate involving another OH^- release, and this intermediate was scavenged by trien. However, this mechanism required a change of species at pH 12.0, and the visible spectrum, the ESR data, and cyclic voltammetric data²³ all show that there is no change of reactant from pH 8.2 to pH 14. Thus, this scheme is not valid, and another restriction is placed upon the proposed mechanism. Other combinations of possible reactions, including the introduction of mixed complexes or variation of the order of steady-state species, would not yield a suitable data fit. The fit of the kinetic data is very sensitive to the reaction sequence selected, and the excellent fit obtained lends credence to the proposed mechanism in eq 12–15.

Kinetics of the Acid Dissociation. The observed first-order rate constants for the acid dissociation of $\text{Cu}(\text{H}_4\text{C})^{2-}$ are presented in Table III. The kinetics obeys the rate expression (17) over the pH interval 4.0–5.3. The value of the gene-

$$k_{\text{obsd}} = k_{\text{H}}[\text{H}^+] + k_{\text{HOAc}}[\text{HOAc}] \quad (17)$$

ral-acid rate constant, k_{HOAc} , can be calculated from the slopes of the buffer dependence plots (Figure 4) by using eq 18 and

$$k_{\text{HOAc}} = \frac{k_{\text{HOAc}}^{\text{T}}(K_{\text{a}} + [\text{H}^+])}{[\text{H}^+]} \quad (18)$$

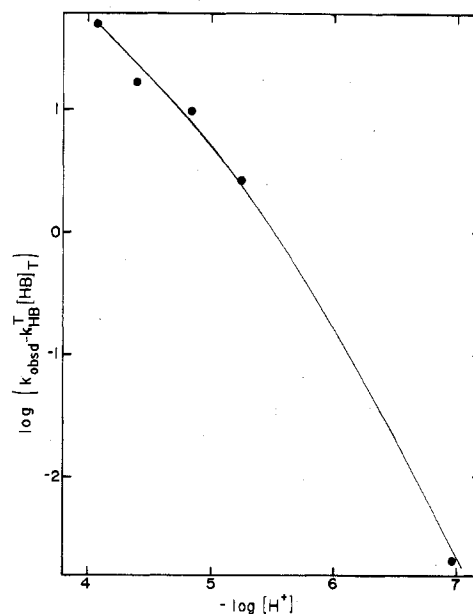
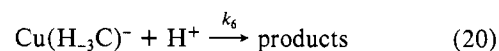
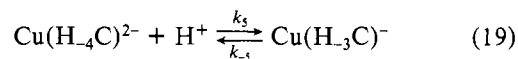


Figure 5. Dependence of k'_{obsd} on $[\text{H}^+]$ for the acid dissociation of $\text{Cu}(\text{H}_4\text{C})^{2-}$ ($[\text{Cu}(\text{H}_4\text{C})^{2-}] = 3.0 \times 10^{-5} \text{ M}$, $\mu = 1.0 \text{ M}$ (NaClO_4), $25.0 \text{ }^\circ\text{C}$). The solid line was calculated from eq 21 with $k_5 = 6.2 \times 10^5 \text{ M}^{-1} \text{ s}^{-1}$ and $k_6/k_{-5} = 3.45 \times 10^5 \text{ M}^{-1}$.

noting that $\text{p}K_{\text{a}}(\text{HOAc}) = 4.61$ at $25.0 \text{ }^\circ\text{C}$ and $\mu = 1.0 \text{ M}$ (NaClO_4).²⁴ Table IV shows that the value of k_{HOAc} is $(4.6 \pm 2.0) \times 10^3 \text{ M}^{-1} \text{ s}^{-1}$. The specific-acid rate constant, $k_{\text{H}} = 6.2 \times 10^5 \text{ M}^{-1} \text{ s}^{-1}$, is determined from the $[\text{H}^+]$ dependence of the intercepts in Figure 4.

The proposed mechanism (eq 19–21) is presented along with



$$k'_{\text{obsd}} = \frac{k_5 k_6 [\text{H}^+]^2}{k_{-5} + k_6 [\text{H}^+]} = k_{\text{obsd}} - k_{\text{HOAc}}[\text{HOAc}] \quad (21)$$

the rate expression. The species, $\text{Cu}(\text{H}_3\text{C})^-$, is a steady-state intermediate in which one of the peptide nitrogens has been protonated. This is the same steady-state species that was found to be subject to nucleophilic attack but needed a second protonation from the solvent before the macrocycle could be displaced. In the acid reaction this species is effectively scavenged by H^+ (eq 20). When $k_6[\text{H}^+] \gg k_{-5}$, eq 21 simplifies to eq 17. The presence of general-acid catalysis means that the rate-determining step is proton transfer to the peptide nitrogen.⁷

As a test of this rate expression, the reaction was conducted at $-\log [\text{H}^+] = 6.98$ in PIPES buffer. Table III presents the observed first-order rate constants. From a plot of k_{obsd} vs. $[\text{PIPES}]_{\text{T}}$, we find a small buffer dependence, $k_{\text{PIPES}}^{\text{T}} = 1.3 \times 10^{-2} \text{ M}^{-1} \text{ s}^{-1}$, and the first-order specific-acid rate constant at this pH, $2.0 \times 10^{-3} \text{ s}^{-1}$. As Figure 5 shows, at low $[\text{H}^+]$ we observe a higher order $[\text{H}^+]$ dependence in accordance with eq 21. The curve in Figure 5 was generated by using the values $k_5 = 6.2 \times 10^5 \text{ M}^{-1} \text{ s}^{-1}$ and $k_6/k_{-5} = 3.45 \times 10^5 \text{ M}^{-1}$.

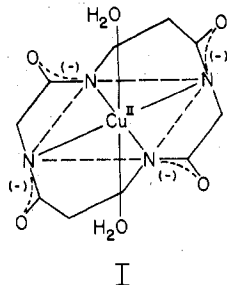
Discussion

The solution structure of the copper(II) complex of the macrocyclic tetrapeptide *cyclo*-(β -alanyl-glycyl- β -alanyl-glycyl) is proposed with the metal chelated to four deprotonated peptide nitrogen atoms in a square-planar geometry (or a

(23) Rybka, J. S.; Margerum, D. W., submitted for publication.

(24) Portanova, R.; DiBernardi, P.; Cassol, A.; Tondello, E.; Magon, L. *Inorg. Chim. Acta* 1974, 8, 233–240.

tetragonally elongated octahedral geometry with water coordinated axially) as in structure I. The room-temperature ESR

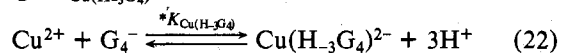


spectrum provides evidence for this assignment. The number of lines due to nitrogen hyperfine coupling shows that there are four equivalent donors in the plane. The ESR spectra of copper(II)-tetraglycine as a function of pH show that both the g value and coupling constants reflect the degree of ligand coordination (i.e., changing with the number of coordinated nitrogens).²⁵ An amino nitrogen and a peptide nitrogen are magnetically equivalent when chelated to copper(II).²¹ The agreement between the g values and coupling constants for $\text{Cu}(\text{H}_4\text{C})^{2-}$ and $\text{Cu}(\text{H}_3\text{G}_4)^{2-}$ is consistent with four deprotonated peptide nitrogen donors. In the anisotropic spectrum, g_{\parallel} is greater than g_{\perp} which is consistent with the metal center in either a square-planar or a tetragonally elongated octahedral geometry.²⁶

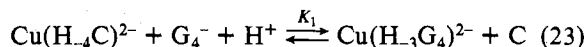
The ESR spectrum of $\text{Cu}(\text{H}_4\text{C})^{2-}$ is characterized by sharp nitrogen hyperfine lines. Similar resolution of the nitrogen coupling is observed for the copper(II) complexes of bis(biuret) and bis(dimethylglyoxime)²⁷ but not for the copper(II) complexes of triglycine or tetraglycine. This effect may be due to the presence of four equivalent nitrogen donor atoms or may indicate that the structure of $\text{Cu}(\text{H}_4\text{C})^{2-}$ is a closer approximation to a square plane than other copper(II) peptide complexes. The crystal structure of $\text{Na}_2\text{Cu}(\text{H}_3\text{G}_4) \cdot 10\text{H}_2\text{O}$ shows the geometry to be nearly square planar with the metal slightly out of the plane.²⁸

The electronic spectrum of $\text{Cu}(\text{H}_4\text{C})^{2-}$ shows one absorbance maximum that corresponds to a copper d-d transition. The energy of this transition has been related to the strength of the ligand donors.²⁹ This scheme predicts $\lambda_{\text{max}} = 520$ nm for a copper(II) chelated by four deprotonated peptide nitrogens. The *N*-formyltriglycylamide complex of copper(II) has donors similar to those of $\text{Cu}(\text{H}_4\text{C})^{2-}$, and its λ_{max} is 507 nm. The copper(II)-macrocyclic peptide complex exhibits a higher energy transition (488 nm) than either of these examples, suggesting that the structure of the ligand is causing more metal-nitrogen interaction. Strain in the two β -alanine rings can account for part of this effect, but the more important consideration is the tightness of the cavity in the 14-membered macrocyclic ligand. Busch has observed that nickel-macrocyclic amine complexes exhibit a larger ligand field splitting as the ring size of the ligand is decreased.³⁰

The stability constant of $\text{Cu}(\text{H}_4\text{C})^{2-}$ was determined to be $\log *K_{\text{Cu}(\text{H}_4\text{C})} = -25.1$ at $\mu = 0.2$ M (NaClO_4). We can compare the stability of the macrocyclic tetrapeptide complex to that of the linear tetrapeptide complex $\text{Cu}(\text{H}_3\text{G}_4)^{2-}$ for which $\log *K_{\text{Cu}(\text{H}_3\text{G}_4)} = -16.31$



For the equilibrium in eq 23, when $[\text{G}_4^-] = [\text{C}]$, there will be



$$K_1 = \frac{[\text{Cu}(\text{H}_3\text{G}_4)^{2-}][\text{C}]}{[\text{Cu}(\text{H}_4\text{C})^{2-}][\text{G}_4^-][\text{H}^+]} = \frac{*K_{\text{Cu}(\text{H}_3\text{G}_4)}}{*K_{\text{Cu}(\text{H}_4\text{C})}} = 10^{9.1} \quad (24)$$

equal concentrations of $\text{Cu}(\text{H}_3\text{G}_4)^{2-}$ and $\text{Cu}(\text{H}_4\text{C})^{2-}$ at pH 9.1. Above pH 9.1 $\text{Cu}(\text{H}_4\text{C})^{2-}$ is favored. A comparison of the relative stability of $\text{Cu}(\text{H}_4\text{C})^{2-}$ with that of the extremely stable Cu^{II} -tet-a complex (tet-a is a 14-membered macrocyclic tetraamine with a stability constant of 10^{28})^{32,33} shows that above 0.35 M OH^- the cyclic tetrapeptide complex would be favored.

The displacement of peptides from their copper(II) complexes has been shown to occur by two general mechanisms involving either nucleophilic attack upon the metal ion or acid attack upon the deprotonated ligand.^{7,10,34,35} The susceptibility to nucleophilic attack by trien is affected by the availability of an equatorial position on the complex. For $\text{Cu}(\text{H}_2\text{G}_3)^-$, only a carboxylate group needs to be displaced in order to make the equatorial site accessible. A rate constant of $1.1 \times 10^7 \text{ M}^{-1} \text{ s}^{-1}$ has been observed for the reaction of this complex with trien.¹⁰ The corresponding rate constant decreases to $500 \text{ M}^{-1} \text{ s}^{-1}$ when the fourth site is occupied by a peptide nitrogen as in $\text{Cu}(\text{H}_3\text{G}_4)^{2-}$ ³⁴ and drops to $0.5 \text{ M}^{-1} \text{ s}^{-1}$ when an imidazole group must be displaced as in $\text{Cu}(\text{H}_2\text{GGhis})^-$.³⁵ In the case of $\text{Cu}(\text{H}_4\text{C})^{2-}$ the attacking nucleophile must displace a peptide nitrogen that is anchored by the cyclic peptide backbone. The direct nucleophilic reaction has a rate constant less than $10^{-5} \text{ M}^{-1} \text{ s}^{-1}$, which is at least 4 orders of magnitude less than that of $\text{Cu}(\text{H}_2\text{GGhis})^-$.

A water-dissociation pathway has been observed for other copper-peptide complexes and is associated with a proton transfer from the solvent to the peptide nitrogen, followed by a rapid scavenging of the intermediate by nucleophiles or solvent. This rate is dependent upon the lability of the peptide nitrogen. For $\text{Cu}(\text{H}_3\text{G}_4)^{2-}$, in which the protonation is at a terminal nitrogen, the observed rate constant is 16 s^{-1} .³⁴ When protonation is at a nonterminal peptide nitrogen as for $\text{Cu}(\text{H}_2\text{G}_3)^-$, where a carboxylate group occupies the terminal position, the rate constant decreases to 0.12 s^{-1} .³⁶ When an imidazole nitrogen is in the terminal position as for $\text{Cu}(\text{H}_2\text{GGhis})^-$, this water-dissociation rate drops to $7.5 \times 10^{-4} \text{ s}^{-1}$.³⁵ In the present study the protonation site for $\text{Cu}(\text{H}_4\text{C})^{2-}$ both is nonterminal and is anchored by a deprotonated peptide nitrogen in the cyclic peptide backbone. The reaction in eq 12 is the water-dissociation pathway with a rate constant of $9.9 \times 10^{-4} \text{ s}^{-1}$ (very similar to that of $\text{Cu}(\text{H}_2\text{GGhis})^-$). We are able to obtain detailed information about this process because $\text{Cu}(\text{H}_4\text{C})^{2-}$ is extremely resistant to nucleophilic attack. Protonation of the complex does not lead to ligand displacement, but it does weaken the square plane sufficiently to allow coordination by trien. The resulting mixed complex requires a second solvent-assisted protonation before trien is able to displace the ligand.

It is apparent that structural considerations of the macrocyclic peptide make direct and solvent-assisted nucleophilic attacks upon the metal unfavorable, leading to a much slower ligand displacement reaction. Similar considerations must be

- (25) Falk, K. E.; Freeman, H. C.; Jansson, J.; Malmstrom, B. G.; Vanngard, T. *J. Am. Chem. Soc.* **1967**, *89*, 6071-6077.
 (26) Drago, R. "Physical Methods in Chemistry"; W. B. Saunders: Philadelphia, PA, 1977; p 484.
 (27) Wiersema, A. K.; Windle, J. J. *J. Phys. Chem.* **1964**, *68*, 2316-2320.
 (28) Freeman, H. C.; Taylor, M. R. *Acta Crystallogr.* **1965**, *18*, 939-952.
 (29) Billo, E. J. *Inorg. Nucl. Chem. Lett.* **1974**, *10*, 613-617.
 (30) Busch, D. H. *Acc. Chem. Res.* **1978**, *11*, 392-400.

- (31) Koltun, W. L.; Roth, R. H.; Gurd, F. R. *N. J. Biol. Chem.* **1963**, *238*, 124-131.
 (32) Curtis, N. F. *J. Chem. Soc.* **1964**, 2644-2650.
 (33) Cabbiness, D. K.; Margerum, D. W. *J. Am. Chem. Soc.* **1969**, *91*, 6540-6541.
 (34) Youngblood, M. P.; Margerum, D. W. *Inorg. Chem.*, in press.
 (35) Wong, L. F.; Cooper, J. C.; Margerum, D. W. *J. Am. Chem. Soc.* **1976**, *98*, 7268-7274.
 (36) Pagenkopf, G. K.; Margerum, D. W. *J. Am. Chem. Soc.* **1968**, *90*, 6963-6967.

Table V. Comparison of Acid, Water, and trien Rate Constants with Copper(II)-Peptide Complexes

copper(II) peptide	k_{H^+} , $\text{M}^{-1} \text{s}^{-1}$	k_{HOAc} , $\text{M}^{-1} \text{s}^{-1}$	$k_{\text{H}_2\text{O}}$, s^{-1}	k_{trien} , $\text{M}^{-1} \text{s}^{-1}$
$\text{Cu}(\text{H}_3\text{G}_4)^{2-}$	1.6×10^8	3.8×10^5	16	4.9×10^2
$\text{Cu}(\text{H}_2\text{G}_3)^-$	1.3×10^7	1.1×10^4	0.12	1.1×10^7
$\text{Cu}(\text{H}_2\text{GGhis})^-$	1.4×10^7	6.3×10^3	7.5×10^{-4}	0.5
$\text{Cu}(\text{H}_4\text{C})^{2-}$	6.2×10^5	4.6×10^3	9.9×10^{-4}	$<10^{-5}$

made in order to account for the observed acid-dissociation kinetics. In general proton-transfer reactions to metal peptide nitrogens are slower than those of "normal" acid-base reactions because of the molecular rearrangements and bond cleavage that must occur in order to make proton transfer complete.⁷ When acid attack is at a terminal peptide nitrogen, as in the case of $\text{Cu}(\text{H}_3\text{G}_4)^{2-}$, the reaction is faster than when protonation occurs at a nonterminal position where the coordinated terminal is retarding the ligand from simply unwrapping and freely leaving. This effect is clearly shown by the order of the specific-acid rate constants, k_{H^+} : $\text{Cu}(\text{H}_3\text{G}_4)^{2-}$ ($1.6 \times 10^8 \text{ M}^{-1} \text{ s}^{-1}$)³⁴ > $\text{Cu}(\text{H}_2\text{GGhis})^-$ ($1.4 \times 10^7 \text{ M}^{-1} \text{ s}^{-1}$)³⁵ \approx $\text{Cu}(\text{H}_2\text{G}_3)^-$ ($1.3 \times 10^7 \text{ M}^{-1} \text{ s}^{-1}$)⁷ > $\text{Cu}(\text{H}_4\text{C})^{2-}$ ($6.2 \times 10^5 \text{ M}^{-1} \text{ s}^{-1}$). For $\text{Cu}(\text{H}_4\text{C})^{2-}$ the ligand is hindered from unwrapping by the structure of the macrocycle. The additional rearrangements involved will easily account for the order of magnitude decrease in k_{H^+} .

The acid reactions of $\text{Cu}(\text{H}_4\text{C})^{2-}$ are general-acid catalyzed which means that the proton step is rate determining. We can compare k_{HOAc} ($\text{M}^{-1} \text{ s}^{-1}$) for the same series of complexes, $\text{Cu}(\text{H}_3\text{G}_4)^{2-}$ (3.8×10^5)³⁴ > $\text{Cu}(\text{H}_2\text{G}_3)^-$ (1.1×10^4)⁷ > $\text{Cu}(\text{H}_2\text{GGhis})^-$ (6.3×10^3)³⁵ \approx $\text{Cu}(\text{H}_4\text{C})^{2-}$ (4.6×10^3), and find that the same structural considerations account for this trend. Comparison of the acid, water, and trien rate constants for these copper-peptide complexes is shown in Table V. The $\text{Cu}(\text{H}_2\text{GGhis})^-$ complex undergoes a different acid-dissociation mechanism and so a direct comparison of k_{HOAc} is unfair. In particular, $\text{Cu}(\text{H}_2\text{GGhis})^-$ forms an intermediate species with the rate-limiting process being a Cu-N bond cleavage. In the presence of trien these intermediates are effectively scavenged and the rate-determining step shifts to the proton transfer.

The nucleophilic reactions of $\text{Cu}(\text{H}_4\text{C})^{2-}$ suggest similarities with $\text{Cu}(\text{H}_2\text{GGhis})^-$ with regard to kinetic stability imparted from the structural considerations of the ligand because both require solvent-assisted protonations. On this basis one would expect the acid reactions to also be similar, but they are quite

different. Other copper(II)-peptide complexes can form stable species with one, two, or three deprotonated groups, but with $\text{Cu}(\text{H}_4\text{C})^{2-}$ we did not find any evidence for stable intermediate species with lower degree of deprotonation. Hence, once one proton adds, the others will follow in rapid succession. This is similar to the behavior of some of the nickel(II)-peptide complexes.³⁷

The acid-dissociation kinetics at higher pH confirm the rate expression of eq 21. Therefore, more than a single proton is required to displace the ligand. This observation is consistent with the nucleophilic reaction (also at higher pH) where two protonations were necessary to drive the reaction.

Conclusions

The solution structure of the copper(II) complex of the macrocyclic tetrapeptide *cyclo*-(β -alanylglycyl- β -alanylglycyl) is determined to be $\text{Cu}(\text{H}_4\text{C})^{2-}$ (structure I) with the metal chelated by four deprotonated peptide nitrogens in a planar arrangement. ESR and visible spectral data suggest that this complex is more square planar (i.e., greater tetragonal distortion) than other copper(II)-linear peptide complexes such as $\text{Cu}(\text{H}_3\text{G}_4)^{2-}$. The macrocyclic peptide complex exhibits increased thermodynamic stability relative to other copper-peptide complexes and has a formation constant $\log *K_{\text{Cu}(\text{H}_4\text{C})} = -25.1$. The complex also shows an increased kinetic stability toward both nucleophilic reactions with trien and acid dissociation. The direct nucleophilic reaction of trien upon the complex is negligible compared to the combined trien and water-dissociation path which consists of a sequence of solvent-assisted protonation, trien coordination, and a second solvent-assisted protonation. The acid-dissociation rates are an order of magnitude slower than for other copper-peptide complexes. The reactions are general-acid catalyzed so that proton transfer to a peptide nitrogen is the rate-determining step. At higher pH the $[\text{H}^+]$ dependence becomes greater than first order. Kinetically, the displacement of a peptide nitrogen is extremely difficult when it is anchored by the macrocyclic peptide backbone and is retarded from leaving the coordination site.

Acknowledgment. This investigation was supported by Public Health Service Grant No. GM 12152 from the National Institute of General Medical Sciences.

Registry No. $\text{Na}_2\text{Cu}(\text{H}_4\text{C})$, 74185-27-6; $\text{Cu}(\text{H}_4\text{C})^{2-}$, 74185-28-7; trien, 112-24-3.

(37) Dorigatti, T. F.; Billo, E. J. *J. Inorg. Nucl. Chem.* **1975**, *37*, 1515-1520.